BOUNDARY-LAYER HEAT AND MOISTURE BUDGETS FROM FIFE

A. K. BETTS[1], R. L. DESJARDINS[2], J. I. MACPHERSON[3], and R. D. KELLY[4]

[1]*RD2, Box 3300, Middlebury, VT 05753, USA*
[2]*Land Resource Research Centre, Agriculture Canada, Ottawa, Ontario, Canada, K1A OC6*
[3]*National Aeronautical Establishment, Ottawa, Ontario, Canada, K1A OR6*
[4]*Dept. of Atmospheric Science, University of Wyoming, P.O. Box 3038, Laramie, WY 82071, USA*

(Received in final form 1 September, 1989)

Abstract. Aircraft stacks were flown upwind and downwind of the First ISLSCP Field Experiment (FIFE) site in Kansas to measure the heat and moisture budgets of the boundary layer under fairly clear skies for four daytime periods. In this paper, we evaluate the terms in the conservation equation. The vertical flux divergence and advection do not account for the difference between surface and low-level aircraft flux estimates. Budget estimates of the surface fluxes using the aircraft data agree well with surface flux measurements, but extrapolation of the aircraft fluxes gives surface fluxes that are too low. With the 5 km cutoff filter used, the aircraft underestimate for sensible heat flux is about 40%, and for the latent heat flux about 30%. Part of the underestimation is attributable to long-wavelength contributions (longer than the 5 km filter), but more investigation is needed.

1. Introduction

The first ISLSCP (International Satellite Land Surface Climatology Project) Field Experiment (hereafter FIFE) took place in 1987 on a 15 km × 15 km grassland ecosystem near Manhattan, Kansas (Sellers *et al.*, 1988). As part of its objectives to develop techniques to quantify the exchange of momentum, heat, moisture and CO_2 between the earth's surface and the atmosphere, FIFE included an extensive program of surface and atmospheric boundary-layer (ABL) measurements. This paper analyzes a series of boundary-layer aircraft flights designed to measure the budgets of heat and moisture for the ABL over the FIFE site for comparison with surface measurements of sensible and latent heat flux. Budget studies over large regions have previously been carried out by several research groups. For example, by using L-shaped flight patterns of approximately 50 km in length at four levels, Lenschow *et al.*, (1981) found that the residual budget terms for sensible and latent heat were small compared to the largest terms in the budget. For ozone, the residual term was assumed to be the photochemical production of ozone. Benech *et al.* (1987) used instrumented systems aboard two aircraft to quantify the contribution of advection and turbulence for sensible and latent heat for a catchment 50 km by 100 km.

The flights in FIFE had three main objectives. The first was to compare tower-based flux measurements from distributed sites with flux profiles in the ABL obtained from line averages using aircraft-based systems. The second was to attempt a volumetric budget of the ABL to assess the importance of horizontal advection terms, and to derive mean surface fluxes for the FIFE area as budget

Boundary-Layer Meteorology **50**: 109–137, 1990.

residuals for a fairly homogeneous ecosystem of the size normally encountered in nature. The third was to check the validity of simple mixed-layer models for the ABL.

These budget studies consisted of 4 or more stacks of east-west runs flown cross-wind over the FIFE site at constant pressure altitudes, separated by 11 km in the north-south direction. Figure 1 shows an example. The purpose was to measure the volumetric budgets of heat and water vapor over the FIFE site by measuring the fluxes at different levels in a relatively cloud-free ABL, together with the time rate of change of temperature and moisture, and advection by the mean wind. Desjardins *et al.*, (1988) presented a preliminary analysis of one of these flights. We shall compare the measurements with the surface flux data, the surface meteorological data from the Portable Automated Meteorological (PAM) stations, and the radiosonde data; and attempt to assess the success of these flights in the context of developing an experimental methodology for obtaining real estimates of energy exchange. These FIFE flights were very informative. They indicate the importance of the fluxes at the boundary-layer (BL) top inversion and the horizontal advection in the BL thermodynamic budget. They show that the budget method can give useful area-averaged surface fluxes, and they generally support the use of mixed boundary-layer models for analysis. However, they also suggest that the surface heat fluxes estimated by extrapolating the aircraft flux profiles are too small in comparison with both the budget estimates and the surface flux measure-

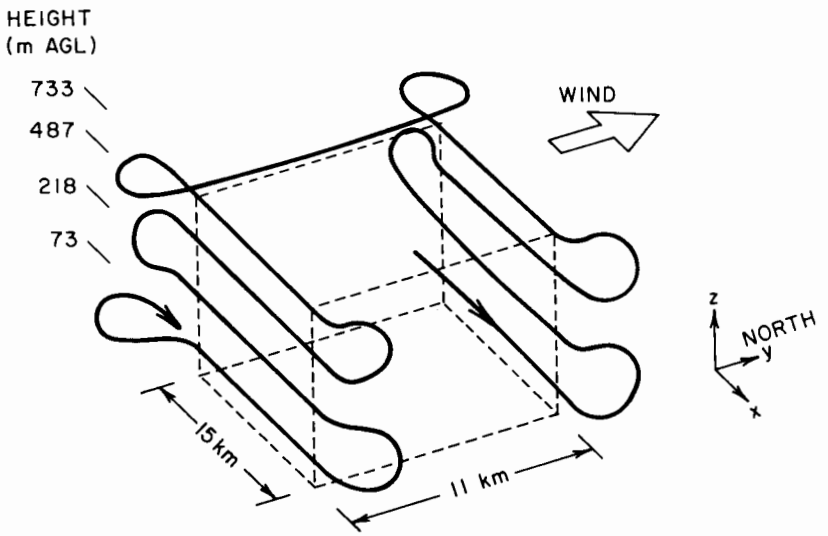

Fig. 1. Double stack flight pattern used by the NAE Twin Otter and UW King Air in heat and moisture budget studies over the FIFE site in 1987. The four levels and orientation illustrated apply specifically to flights on October 8. Different levels were used on other days.

ments. The reasons for this are still being investigated, but are thought to include long-wavelength contributions to flux densities.

2. Instrumentation

Two aircraft were used for these flights. The Canadian National Aeronautical Establishment Twin Otter (abbreviated NAE TW in the tables), an atmospheric research aircraft, was instrumented to measure the three orthogonal components of atmospheric motion, air temperature, CO_2 and water vapor fluctations (MacPherson *et al.*, 1985). It was also instrumented with a slow response Cambridge dew-point system for humidity measurements. All signals are sampled at 16 Hz, low pass filtered at 5 Hz and high pass filtered at 0.012 Hz. This corresponds to spatial scales from about 10 m to 5 km at an aircraft speed of 50 m s^{-1}. The data recording and processing followed the procedures discussed in Desjardins *et al.* (1989a). The 0.012 Hz high pass filter was used to minimize the variability from run to run. Even though it can lead to a slight underestimate of the turbulent fluxes (Desjardins *et al.*, 1984), it is essential when comparing short flight legs as in this study.

The University of Wyoming King Air (abbreviated UW KA in the tables) research aircraft was likewise instrumented for measurements of air motion (gust probe and inertial navigation system), air temperature (Rosemount unheated temperature probe), and water vapor (Cambridge dew-point hygrometer and Wyoming Lyman-alpha hygrometer). All signals used in the eddy-correlation flux calculations (gust probe, temperature, pressure, Lyman-alpha) were sampled at 10 Hz and low-pass filtered at 2 Hz before recording. Prior to the analysis presented here, the high-rate (10 Hz) data were high-pass filtered at 0.017 Hz (5 m wavelength) using a third-order recursive filter (Jacquot, 1981; Budak, 1974). The Lyman-alpha values were calibrated against the low-rate dew-point values (1 Hz) by using data from the take-off sounding of each flight. Vertical fluxes of latent heat for both aircraft were subsequently corrected for the effects of sensible heat flux following Webb *et al.* (1980).

3. Methodology

a. Flight plan

A typical flight plan is shown in Figure 1 (for October 8, 1987). Both the Twin Otter and the King Air flew sixteen 15 km runs in an east-west direction along two tracks 11 km apart over the FIFE site in Kansas. For the Twin Otter, these consisted of four runs at the north edge at approximately 75, 220, 500 and 740 m AGL (above ground level); then eight runs at the south edge at 740, 500, 220, 75, 75, 220, 500 and 740 m; then four more runs at the north edge at 740, 500, 220 and 75 m. The actual altitudes varied slightly. A similar King Air flight pattern was flown at the same time, but it started and ended with 75 m AGL runs along

the south end of the site. These runs were made between 1810 and 2040 UTC during reasonably clear conditions and with strong winds from the south. The order of the runs was selected such that the average time of any two corresponding passes at each altitude was the same. Using a single aircraft with one set of sensors simplifies the task of measuring horizontal gradients, provided the sensors do not drift with time. It is difficult, however, to measure spatial derivatives accurately in a rapidly changing situation. The stacks were flown so that the stack pairs at the north end of the site were flown close to the same average time as at the south end, and a correction can be made for the small difference in time. However, it is still necessary in the budget analysis to assume a linear trend with time, and constant advection for roughly two hours.

B. Summary of flights

Table I summarizes the flights analyzed in this paper, together with the mean inversion height and Bowen ratio (determined by radiosonde and aircraft soundings) and the surface Bowen ratio from the surface flux measurements. Four of the flights were flown by the NAE Twin Otter and two by the UW King Air. Three were in August when the surface vegetation was actively growing and the surface Bowen ratio was low, and three in October after the vegetation had largely died, and the surface Bowen ratio was high.

C. Budget analysis

The budget equation for a conserved scalar, S, for which there are no sources and sinks in the boundary layer, can be written:

$$\partial\bar{S}/\partial t + \bar{u}\,\partial\bar{S}/\partial x + \bar{v}\,\partial\bar{S}/\partial y + \bar{w}\,\partial\bar{S}/\partial z + \partial(\overline{u'S'})/\partial x + \partial(\overline{v'S'})/\partial y + \partial(\overline{w'S'})/\partial z = 0\,, \tag{1}$$

where $\bar{u}$, $\bar{v}$, and $\bar{w}$ are the three wind components along the x, y, and z directions, oriented in the conventional meteorological directions: to the East, North, and upward, respectively. Equation (1) has a time rate-of-change term, mean advection terms, and eddy transports by the boundary-layer turbulence. Overbars denote

TABLE I

Flight data for advection budgets

Aircraft	Flight No.	Date	Time UTC	Surface BR	Mean wind (°/m s^{-1})	Inversion Height (m)	Inversion BR
NAE TW	29	Aug. 20	1720–1925	0.31	191/11.0	500	−0.40
NAE TW	30	Aug. 20	2050–2220	0.12	187/13.5	700	−0.28
NAE TW	36	Oct. 8	1810–2040	3.7	177/12.4	1050	+4.0
NAE TW	41	Oct. 13	1720–1925	3.9	190/11.8	850	−0.32
UW KA		Aug. 20	1720–1920	0.31	187/11.9	500	−0.4
UW KA		Oct. 8	1800–2000	4.0	175/12.3	1000	+4.0

horizontal averaging, and primes indicate deviations from the horizontal average. Three terms in Equation (1) will be dropped. The vertical advection $\bar{w}\,\partial\bar{S}/\partial z$, will be neglected, since estimates show it to be an order of magnitude smaller than any other term, because $\bar{w}$, (estimated from the horizontal divergence) is small, and $\partial\bar{S}/\partial z$ is small in the nearly mixed BL (Desjardins *et al.*, 1988). The horizontal divergence of the horizontal eddy fluxes have been estimated by using the aircraft data, and they are also negligible. Equation (1) then reduces to:

$$\partial\bar{S}/\partial t + \bar{u}\,\partial\bar{S}/\partial x + \bar{v}\,\partial\bar{S}/\partial y + \partial(\overline{w'S'})/\partial z = 0\,. \tag{2}$$

We shall present layer-averaged budgets for potential temperature, θ, and mixing ratio, q. The aircraft made flux runs at three or four levels, so that we can estimate the vertical flux divergence between the lowest and highest aircraft levels. A separate estimate will be made using the flux difference between the highest aircraft level and the average of the surface flux stations. The time rate of change will be found from the time sequence of stack averages. The along-wind advection will be found from the difference between the stacks at the south and north of the pattern corrected for any difference in mean time using the time trend. The predominantly cross-wind advection, $\bar{u}\,\partial\bar{S}/\partial x$ (which is along the flight legs) will be found from averaging the values for all the legs, using the mean trend line for each leg for the gradient, $\partial\bar{S}/\partial x$.

We shall use Equation (2) in three ways. We first calculate all terms using only the aircraft data and find the residual. Then we recalculate the flux divergence term using the surface data and the highest-level aircraft data, and compare the residual. Finally, using again the highest-level aircraft data, we find the surface flux and flux divergence which would give no residual: we call this the budget estimate of the surface flux. In essence, given the fluxes (measured by aircraft) through the top of the volume, defined by the surface and the two stacks in Figure 1, and the time rate of change and advection terms from the aircraft measurements, we can integrate Equation (2) downward to find budget estimates for the mean surface fluxes.

D. Advection time-scale

The accuracy of the estimate of the along-wind (south to north) advection term is, however, not as good as that of the time derivative and cross-wind advection, because the corresponding time-scale is smaller. Typically, $u \approx 2\,\mathrm{m\,s^{-1}}$ and $v \approx 12\,\mathrm{m\,s^{-1}}$ for the patterns shown in Figure 1.

Time-scale of $\partial/\partial t \approx (1/5000)\,\mathrm{s^{-1}}$,
Time-scale of $\bar{u}\partial/\partial x \approx (1/7500)\,\mathrm{s^{-1}}$,
Time-scale of $\bar{v}\partial/\partial y \approx (1/900)\,\mathrm{s^{-1}}$.

This means that air takes only 15 min to pass across the area: a consequence of the high southerly wind speed ($\sim 12\,\mathrm{m\,s^{-1}}$) and the short distance between the

TABLE II

Accuracy of Budget Terms: θ Budget

$(\bar{\rho}C_p x)$	$\partial\theta/\partial t$	$\bar{u}\,\partial\theta/\partial x$	$\bar{v}\,\partial\theta/\partial y$	$\partial(\overline{w'\theta'}/\partial z)$	Residual	Units
Error	±0.018	±0.02	±0.086	(±0.030)	±0.10	W m^{-3}

stacks (≈11 km). For future experiments, it is desirable to at least double the along-wind distance between stacks.

E. Budget accuracy

Assessing the accuracy of the budgets is not straightforward. In the figures we shall present the individual leg means as well as their averages, as a visual guide to the variability of the data. Comparison between the two aircraft and corresponding budgets on different days gives a further insight in support of the error estimates we present here. Table II summarizes our general assessment of the accuracy in W m^{-3} of individual terms in Equation (2) and later tables.

The time rate of change error is based on a ±0.1 K error in the change of θ over a 2-h period. Figures 2, 7, and 11 suggest that this is a reasonable error if allowance is made for the time and height trends of θ. The cross-wind advection error is easier to assess because 16 or more legs are available with a corresponding mean and a variance typically ±0.02 W m^{-3} as shown. The along-wind advection is the term with the largest error because the advection distance and time are so short (see 3(d) and Lenschow, 1970; Lenschow *et al.*, 1981). We used a smaller estimated error in $\delta\theta$ of ±0.07 K, reduced by $1/\sqrt{2}$ because this term is typically based on twice as much aircraft data as the rate-of-change term. The vertical flux divergence error depends on both the probable error in the fluxes (typically ±20% of their value) and the spacing of the aircraft stacks (200–650 m): we give a typical value corresponding to ±20 W m^{-2} in the flux difference, and 650 m between highest and lowest aircraft legs. This error does not include biases due to using high and low pass filters. One concludes from Table II that budget residuals less than 0.10 W m^{-3} may not be significant. This corresponds to an error in the budget estimate of the surface flux of 75 W m^{-2} for the deeper aircraft stacks (October 8, 13). The terms in the moisture budget have similar accuracies in the same units of W m^{-3}. However, when compared with the surface data, most of the budgets appear slightly better than this error analysis would suggest.

The neglect of the radiative cooling of the ABL (≈1 K day^{-1} during the daytime) introduces a small systematic error of about +0.01 W m^{-3} into the θ budgets, about an order of magnitude less than the error from the measurements.

4. Results

We shall present each of the days separately, starting with October 8, 1987, the flight pattern shown in Figure 1.

A. October 8 budget

(i) *Time Rate of Change*

Both aircraft flew this mission, alternating at the north and south ends of the pattern. Figure 2 shows the trend of potential temperature, θ, with time as obtained from the 2 aircraft, an average of 8 PAM surface stations and four radiosondes (labeled R) vertically averaged from 10 to 750 m. The agreement is satisfactory. The Canadian Twin Otter is systematically warmer by 0.25 K than the Wyoming King Air, but the aircraft trends (through the stack means) agree closely. The radiosonde means are comparable, considering that each sensor has an accuracy of ±0.5 K, and each ascent is only a 3 min sample. The surface data show a similar trend (warmer as expected in the superadiabatic layer), with a little more

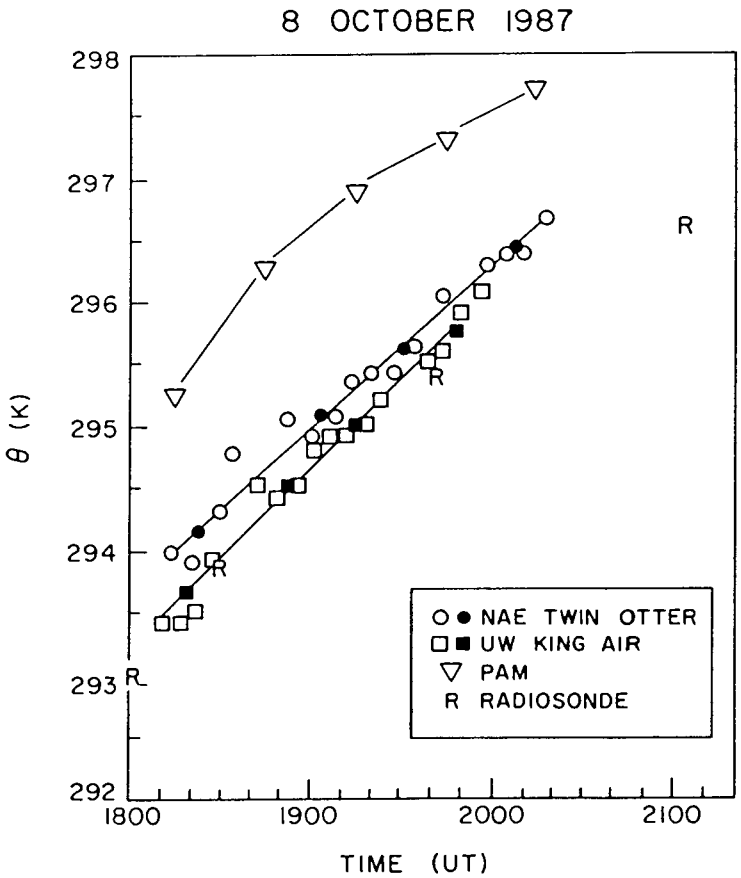

Fig. 2. Changes in potential temperature with time for measurements on October 8, 1987 from four different sources: surface mesonet (PAM, open triangles); pass-averages (open circles) and stack-averages (solid circles) from NAE Twin Otter; pass-averages (open squares) and stack-averages (solid squares) from UW King Air; and four FIFE radiosondes ("R").

curvature. This may be associated with the maximum in surface temperature at local noon (1900 UTC).

Figure 3 shows the corresponding trend of mixing ratio, q, with time. Here there is a wide disparity between the aircraft. The Twin Otter trend closely follows the surface data in the slightly moister superadiabatic layer. The sonde data of lower accuracy and representivity (each sonde has a different sensor) are roughly comparable. However, the King Air data are too moist in absolute terms, show an increasing trend with time, and reveal a much larger gradient with height than the Twin Otter data. The non-linear trend in the King Air data suggests sensor drift and perhaps height bias. For this reason, moisture and latent heat budgets were not attempted with these measurements.

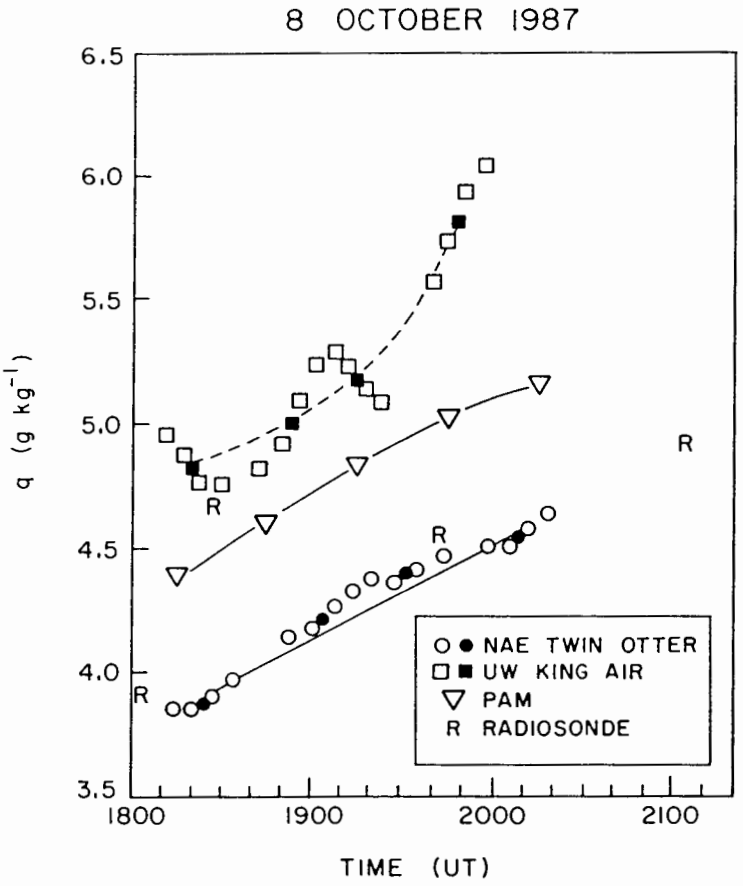

Fig. 3. Changes in mixing ratio with time for measurements on October 8 from four different sources: surface mesonet (PAM, open triangles); pass-averages (open circles) and stack-averages (solid circles) from NAE Twin Otter; pass-averages (open squares) and stack-averages (solid squares) from UW King Air; and four FIFE radiosondes ("R").

(ii) *Heat and Moisture Fluxes*

Figures 4 and 5 show profiles of sensible and latent heat fluxes with height for the NAE Twin Otter, together with mean values for each flight level. They also show three surface values: one measured at the surface (denoted S) as an average of the surface eddy correlation and Bowen ratio sites; a linear extrapolation (long-dashed line) of the aircraft data (denoted A) using the lowest and highest level flux averages; and a value derived from the budget (denoted B) which is discussed below. The mean inversion height was 1050 ± 100 m, and estimates of the fluxes at this level (labeled I) were calculated from a mixed-layer model, also discussed below. Clearly other linear or non-linear fits could be made to the aircraft data. The mean profile has some curvature, and a non-linear extrapolation to the surface (short dashes) would give a slightly higher surface flux estimate (A'). However, both A and A' are far less than the mean surface measurement S. At the highest

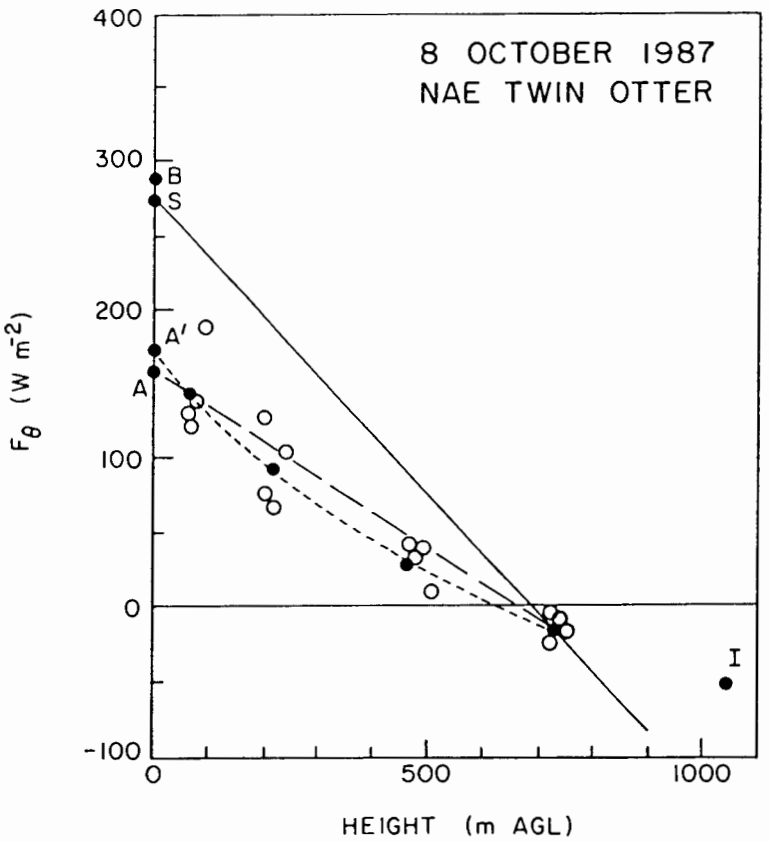

Fig. 4. Sensible heat flux values as functions of height based on budget analysis of the NAE Twin Otter data from 1810 to 2040 UTC, October 8, 1987. The solid-circle values labeled "B," "S," "A," "A'," and "I" are explained in the text. The remaining solid-circle points are level-average fluxes; the open circles are pass-average fluxes.

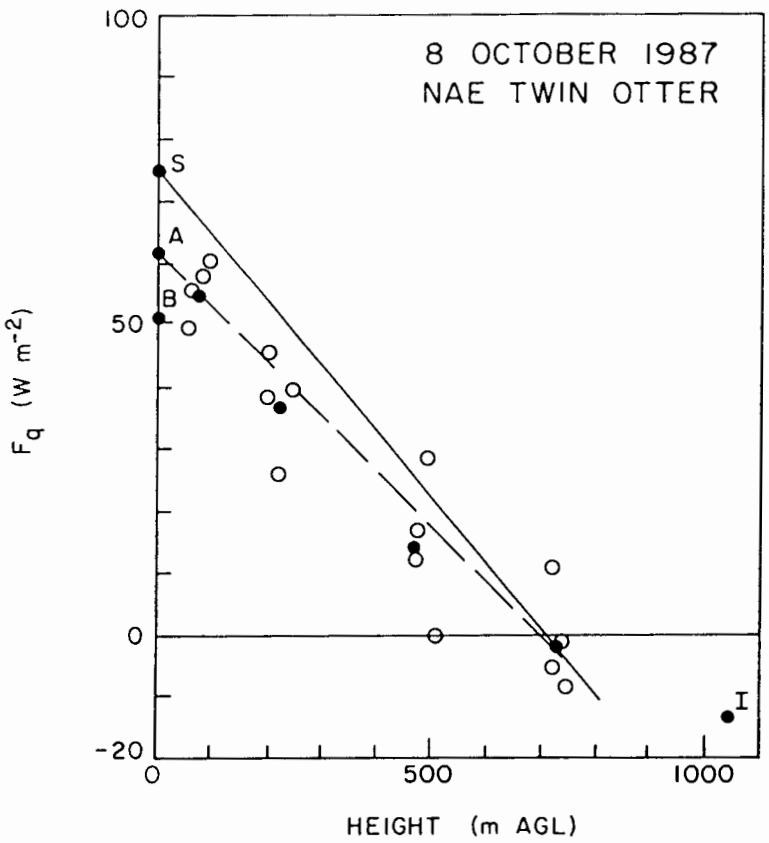

Fig. 5. Latent heat flux values as functions of height based on budget analysis of the NAE Twin Otter data from 1810 to 2040 UTC, October 8, 1987. The solid-circle values labeled "*B*," "*S*," "*A*," and "*I*" are explained in the text. The remaining solid-circle points are level-average fluxes; the open circles are pass-average fluxes.

level, the aircraft heat fluxes are small. This is typically always true of the sensible heat flux, which becomes negative at or below the inversion (see Appendix), and on October 8 it was also true of the latent heat flux, because there was little gradient of moisture across the inversion, where entrainment was occurring. We used the aircraft data from Figures 2, 3, and 4 to perform a volume budget computation for the FIFE site from the surface to the highest aircraft level near 740 m.

Figure 6 shows the heat fluxes measured by the University of Wyoming aircraft, flown at a slightly earlier mean time, when the inversion was a little lower (Table I), and the measured surface heat flux (*S*) a little higher. The linear extrapolation of the aircraft data is also higher (*A*), but still less than *S*. The budget estimate of the surface heat flux (*B*) is much higher and questionable (see below).

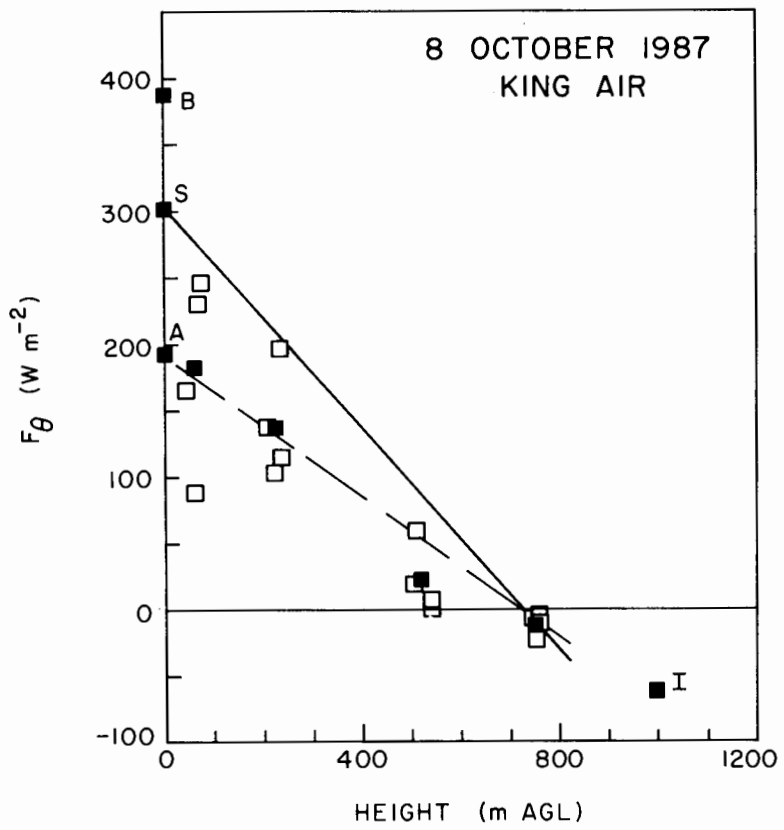

Fig. 6. Sensible heat flux values as functions of height based on budget analysis of the UW King Air data from 1810–2000 UTC, October 8, 1987. The solid-square values labeled "*B*," "*S*," "*A*," "*A'*," and "*I*" are explained in the text. The remaining solid-square points are level-average fluxes; the open squares are pass-average fluxes.

(iii) *Inversion Level Fluxes*

Figures 4 to 6 also show inversion level fluxes (I), estimated from dry mixed-layer model theory. Details are in the Appendix. The Bowen ratio at the inversion, β_I, was estimated from the slope of $\partial\bar{\theta}/\partial\bar{q}$ across the inversion as ~4 (Table I). There is a considerable variation (from 2 to 10) because, although there is a strong temperature inversion, there is a very small increase in mixing ratio across the BL top. For the Twin Otter data in Figure 4, using (A4a):

$$F_{I\theta} = -55 \text{ W m}^{-2} \quad \text{for} \quad F_{0\theta} = 286 \text{ W m}^{-2},$$

where $F_{0\theta}$, $F_{I\theta}$ denote the surface and inversion heat fluxes. Appendix (A4b) then gives an estimate of the latent heat flux at the inversion base as

$$F_{Iq} = -55/\beta_I = -14 \text{ W m}^{-2}.$$

For the King Air data in Figure 6, where the mean surface flux is 298 W m^{-1}, $F_{1\theta}$ = −61 W m^{-2}. The virtual heat flux correction is here almost negligible. Figures 4 to 6 show that the inversion-level fluxes from this model are somewhat less than found by extrapolating the solid line to the inversion level, suggesting a higher value of the closure parameter k, defined in the Appendix.

(iv) *Heat and Moisture Budgets*

Table III shows three summary budgets for October 8: the θ budgets from the two aircraft and the moisture budget from the NAE Twin Otter. The four terms in Equation (2) are shown, as well as a residual. The first term, the time rate of change, is found from the average of the first and last aircraft stacks (about 90 min apart in time). The mean wind was 177/12.4 m s^{-1} (from slightly east of south). The second term is the cross-wind advection; it is the average of the values for all 16 legs, and it is small. The third term is the along-wind advection. The north-south gradient is found by averaging all the northern and southern legs, and correcting for the small difference in mean time (here about 2 min) using the mean time trend. The NAE aircraft showed a small value for this $\bar{\theta}$ advection. As discussed in section 3(c), we estimated the vertical advection in the ABL, using $\partial\bar{u}/\partial x$ and $\partial\bar{v}/\partial y$ to find $\bar{w}$, and found it to be an order of magnitude smaller than even the small x advection; therefore it was neglected. We also estimated the horizontal divergence of the horizontal eddy flux, and found it too was negligible.

Two values are shown for the vertical divergence of the eddy heat and moisture fluxes: they are labeled aircraft/surface. The first uses the difference of the lowest and highest aircraft mean fluxes (the slope of the long dashed line in Figures 4–6); the second uses the difference between the measured surface data and the highest-level aircraft data (the solid line in Figures 4–6). The sum of these four terms in

TABLE III

Heat and moisture budgets for October 8, 1987

θ Budget ($\bar{\rho}C_p x$)	$\partial\bar{\theta}/\partial t$	$\bar{u}\,\partial\bar{\theta}/\partial x$	$\bar{v}\,\partial\bar{\theta}/\partial y$	Aircraft/surface $\partial(\overline{w'\theta'})/\partial z$	Aircraft/surface Residual	Units
NAE TW	0.405	0.021	−0.016	−0.239/−0.392	0.171/0.028	W m^{-3}
		Residual as layer flux difference (R_A/R_S)			125/13	W m^{-2}
		Surface flux (budget/aircraft/surface)			286/161/273	W m^{-2}
UW KA	0.446	0.028	0.062	−0.270/−0.412	0.266/0.124	W m^{-3}
		Residual as layer flux difference			195/91	W m^{-2}
		Surface flux (budget/aircraft/surface)			389/194/298	W m^{-2}
q Budget ($\bar{\rho}Lx$)	$\partial\bar{q}/\partial t$	$\bar{u}\,\partial\bar{q}/\partial x$	$\bar{v}\,\partial\bar{q}/\partial y$	$\partial(\overline{w'q'})/\partial z$	Residual	Units
NAE TW	0.296	0.019	−0.245	−0.086/−0.103	−0.016/−0.033	W m^{-3}
		Residual as layer flux difference			−12/−24	W m^{-2}
		Surface flux (budget/aircraft/surface)			50/61/74	W m^{-2}

Equation (2) for the time change, horizontal advection and vertical eddy flux divergence is the residual error in the budget in $W\,m^{-3}$. Multiplying by the mean height of the highest aircraft legs (733 m) converts these residuals to flux residuals in $W\,m^{-2}$. We get two residuals: R_A, and R_S, using the aircraft and surface values for the vertical flux divergence.

The third line of each budget gives three surface fluxes corresponding to the points B, A, S in Figures 4–6. These were found as follows:

$$B = S + R_S\,, \tag{3a}$$

$$A = B - R_A\,. \tag{3b}$$

The budget value (B) is the surface flux which would give zero residual: it is the estimate of the mean FIFE surface flux from integrating Equation (2), using the aircraft data for the time change, advection and fluxes at 733 m. The aircraft value (A) represents a linear extrapolation of the aircraft flux divergence down to the surface. We see that the budget estimate (B) of the surface θ flux for the NAE Twin Otter (Figure 4) is close to the measured surface mean value (S), whereas the aircraft surface estimate (A) is $\sim 110\,W\,m^{-2}$ lower. For the UW King Air budget (Figure 6) at a slightly earlier time, A is also $\sim 100\,W\,m^{-2}$ below S, but B is $\sim 90\,W\,m^{-2}$ greater than S. In comparison with the Twin Otter budget, the King Air θ budget shows higher values of the time rate of change and vertical flux divergence, but these are at least partly due to the earlier average time, centered on local noon. However, the King Air estimate of the advection $v\,\partial\theta/\partial y$ is larger, and both residuals are also larger than the Twin Otter budget. More than 60% of this difference in residuals is in fact accounted for by the difference in this advection term, the least accurately known term (see Table II). We believe that the resulting budget estimate of the surface θ flux from the King Air data is too large in this case.

The last budget in Table II is the moisture budget from the NAE Twin Otter. It is clear from the aircraft and surface data that the FIFE volume is moistening, although the vertical moisture flux divergence is small. The budget shows that advection of moisture from the south is responsible. The residuals are small, and certainly within the (poorly known) errors of the budget. The aircraft-extrapolated flux is a little lower than the surface measurements, whereas the budget estimate is lower still. However all these latent heat fluxes are low because the surface vegetation is largely senescent, and the soil surface is dry.

B. October 13 budget

A similar flight plan was flown by the NAE Twin Otter on October 13. Surface conditions were similar with a high Bowen ratio, but, in contrast to October 8, there was a sharp fall of mixing ratio at the inversion, and correspondingly (with entrainment of dry air at the inversion) the latent heat flux increased with height, giving a small negative Bowen ratio at the inversion (Table I).

(i) *Time Rate of Change*

Figure 7 shows the time trend of $\overline{\theta}$ for the aircraft legs, the surface meteorological stations and two points for radiosonde means. This budget study is complicated by the presence of clouds over the FIFE area from approximately 1820 to 1900 UTC. The warming of the surface ceased, the mean surface fluxes over the FIFE area fell by 30% (not shown) and 4 aircraft legs at the north end showed greatly reduced fluxes (Figures 9, 10). Figure 8 shows the trend of q with time. The surface and aircraft data show a drying trend, but moister, cooler air appears to be over the site around 1840 UTC under the clouds. This is consistent with the drop in the surface flux of heat, and in the moisture flux divergence associated with entrainment of dry air at the inversion.

(ii) *Heat and Moisture Fluxes*

Figures 9 and 10 are similar to Figures 4 and 5. The mean inversion height was a little lower, near 850 ± 100 m. The flux runs of stack 3, and the last and lowest

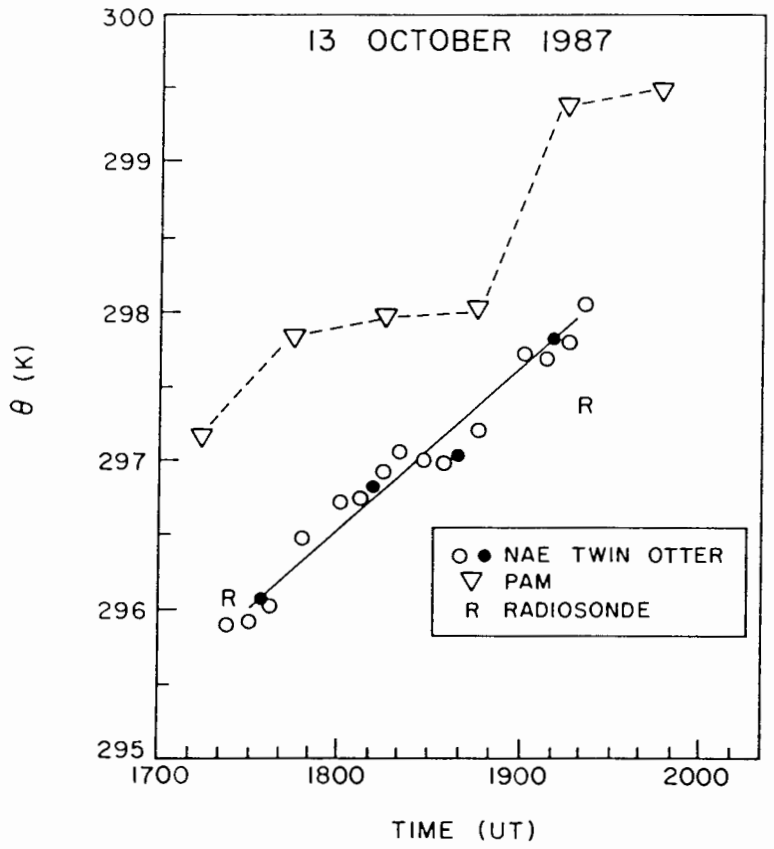

Fig. 7. Changes in potential temperature with time for measurements on October 13, 1987. See Figure 2 for interpretation of symbols.

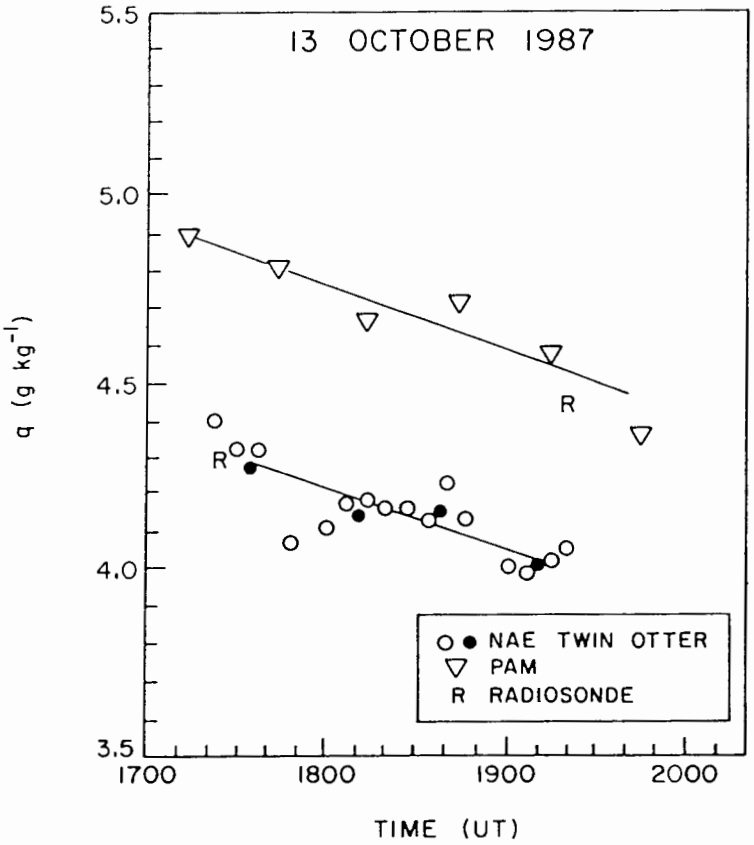

Fig. 8. Changes in mixing ratio with time for measurements on October 13, 1987. See Figure 3 for interpretation of symbols.

run of stack 2 (bracketed open circles) were under cloud, and have been excluded from the flux averages. The dashed and solid lines (coincident in Figure 10) show the vertical flux gradients used in the budget: the moisture flux increasing with height is associated with the entrainment of dry air at the inversion. The measured surface θ flux, S, and B, the budget estimate, are again much larger ($\sim$140 W m^{-2}) than the linear extrapolation of the aircraft profile to the surface. However, all three surface estimates agree closely for the latent heat flux (which is small).

(iii) *Inversion-Level Fluxes*

Figures 9 and 10 also show inversion-level flux estimates from the mixed-layer model (see Appendix). The inversion level height was approximately 850 $\pm$ 100 m during the aircraft pattern, and the Bowen ratio at the inversion β_I was -0.32 ($\pm$0.05) from the two radiosondes at 1727 and 1922 UTC and one aircraft sound-

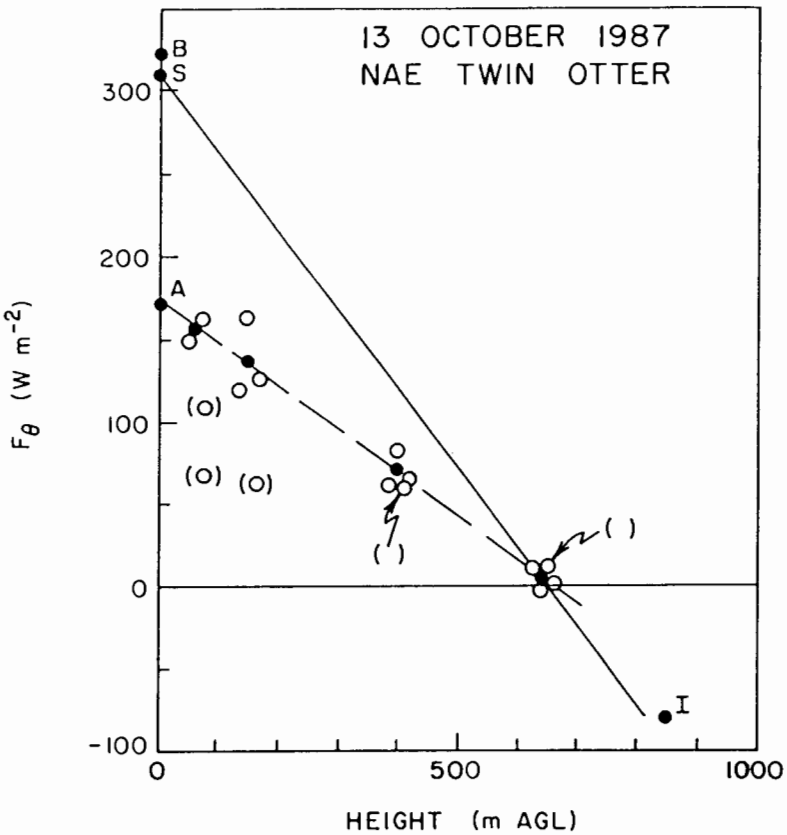

Fig. 9. As in Figure 4, for Twin Otter data from 1720 to 1925 UTC on October 13, 1987. Data points in parentheses were excluded from this budget.

ing. Equations (A4a) and (A4b) give

$$F_{1\theta} = -0.2 \times 312 \times (1.02/0.785) = -81 \text{ W m}^{-2}$$
$$F_{1q} = 253 \text{ W m}^{-2}.$$

Figures 9 and 10 show that these values are roughly consistent with extrapolating the solid flux profiles to the inversion height. The upward moisture flux at the inversion level is nearly three times that at the surface. The entrainment velocity corresponding to these fluxes is $\approx$2 cm s^{-1}; but we do not have sufficiently accurate measurements of ABL depth to check this independently.

(iv) *Heat and Moisture Budgets*

We analyzed the budget entirely excluding the aircraft stack 3 at the north end of the FIFE site, which is the one primarily contaminated by the advection of clouds over the FIFE site. Because the advection time over the site was short (~20 min), the other 3 stacks seem unaffected by cloud (except the fluxes from the last and

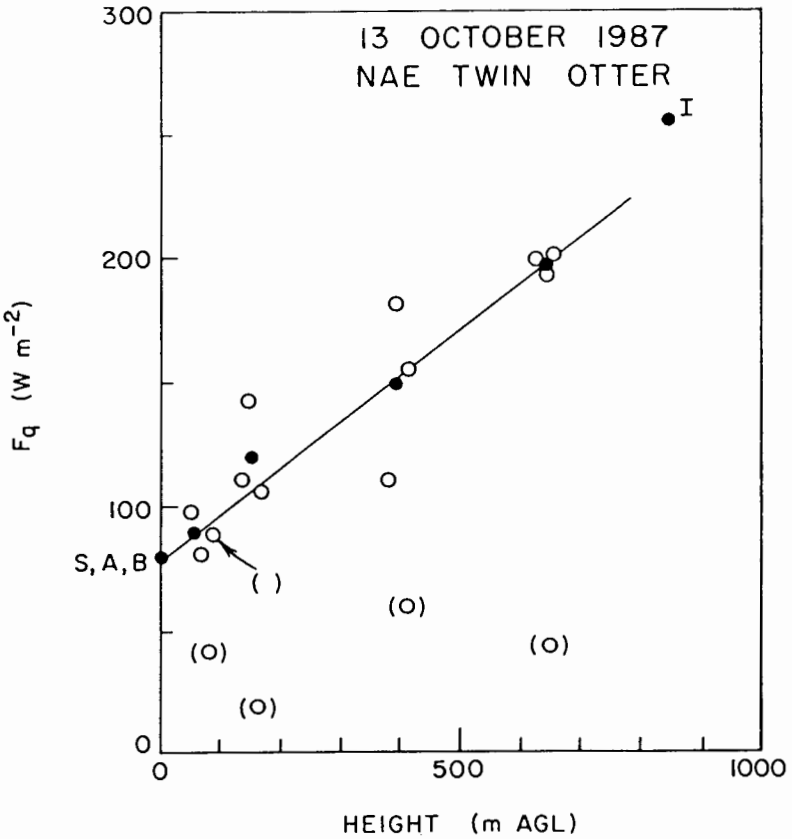

Fig. 10. As in Figure 5, for Twin Otter data from 1720–1925 UTC on October 13, 1987. Data points in parentheses were excluded from this budget.

TABLE IV

Heat and moisture budgets for October 13, 1987

θ Budget				Aircraft/surface	Aircraft/surface	
$(\bar{\rho}C_p x)$	$\partial\theta/\partial t$	$\bar{u}\,\partial\theta/\partial x$	$\bar{v}\,\partial\theta/\partial y$	$\partial(\overline{w'\theta'})/\partial z$	Residual	Units
NAE TW	0.339	0.004	0.156	−0.259/−0.478	0.240/0.021	W m^{-3}
			Residual as layer flux difference		154/13	W m^{-2}
			Surface flux (budget/aircraft/surface)		320/167/307	W m^{-2}
q Budget						
$(\bar{\rho}L\,x)$	$\partial\bar{q}/\partial t$	$\bar{u}\,\partial\bar{q}/\partial x$	$\bar{v}\,\partial\bar{q}/\partial y$	$\partial(\overline{w'q'})/\partial z$	Residual	
NAE TW	−0.128	0.038	−0.092	0.186/0.184	0.004/0.002	W m^{-3}
			Residual as layer flux difference		+3/+1	W m^{-2}
			Surface flux (budget/aircraft/surface)		79/77/78	W m^{-2}

lowest leg of stack 2, which was also excluded from the flux mean in Figures 9 and 10). We shall compute the advection terms from stacks 1, 2, and 4 only. Since the advection terms are the least accurate, this does introduce greater uncertainty into the budget, but the budgets appear satisfactory, and they show surface fluxes consistent with those on October 8. Table IV shows the heat and moisture budgets for October 13.

The cold air advection, based on the offset of stack 2 from the trend line in Figure 7 is a significant term in the budget. The budget is nearly in balance using a surface heat flux of 307 W m^{-2} (which excludes the surface fluxes during the cloudy period), but as on October 8, the aircraft θ fluxes at the lowest level are too small to balance the budget. Figure 9 shows the heat flux profiles, with a dashed line through the aircraft means for the cloud-free legs extrapolated to a surface value $A \approx 167$ W m^{-2}, about 140 W m^{-2} less than the average of the surface flux measurements, S. This discrepancy is similar to that of October 8. The budget estimate, B, of the surface heat flux is 320 W m^{-2} (Table IV), close to the measured surface value.

The drying of the layer is less than that associated with the vertical flux divergence because there is significant moist advection from the south. The residuals are far too small to be significant. The measured surface flux (78 W m^{-2}) agrees with the aircraft flux data extrapolated to the surface. We conclude that the latent heat flux profile measured by aircraft with the moisture flux increasing with height is consistent with the budget. The drying of the layer is driven by the entrainment of dry air into the ABL, partly offset by the moist advection.

c. August 20 budget

Two Twin Otter and one King Air advection patterns were flown on August 20, when the surface evapotranspiration was large. For all three patterns, only three flight levels were flown. For the first Twin Otter mission (1705–1840 UTC), 12 legs were flown at the north end of the FIFE site and 6 at the south. For the second Twin Otter flight (2050–2230 UTC), 6 legs were flown at each end of the FIFE site. The King Air flight (1720–1920 UTC) included 12 legs at the south end and 6 legs at the north end of the FIFE site.

(i) *Time Rate of Change*

Figure 11 shows the time trend for all of the aircraft legs, the average of the surface PAM stations, and five radiosonde sounding averages. The first two flights were before local noon and the third after the surface temperature maximum. Clearly, accurate gradients cannot be found from the five radiosondes, where each sensor is accurate to ±0.5 K. The trend of the surface data and the aircraft legs agree well during the morning temperature rise, but, not in the afternoon when the surface superadiabatic layer weakened. Figure 12 shows the time trend of mixing ratio q for the Twin Otter. Surface and aircraft again tracked well during the morning, but not during the afternoon. There is some lack of continuity

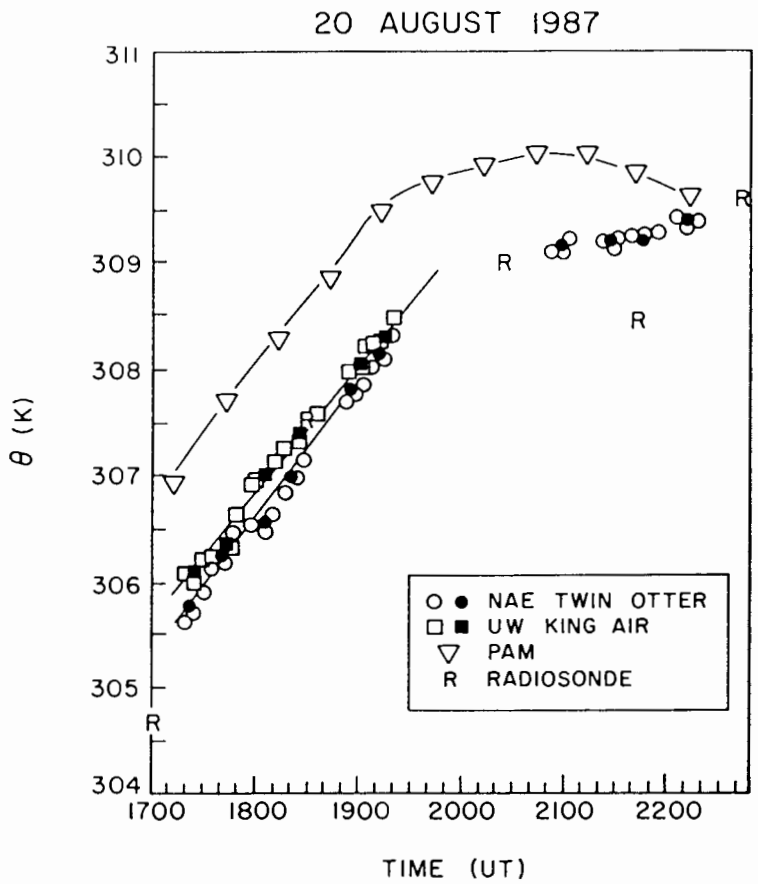

Fig. 11. Changes in potential temperature with time for measurements on August 20, 1987. See Figure 2 for interpretation of symbols.

between the morning and afternoon flights, for which we have no explanation. The mean time changes (lines shown) were found from differencing the average of stacks 5 and 6 from stacks 1 and 2, for the morning flight, and stack 4 from stack 1 for the afternoon (all at the north end of the site).

(ii) *Heat and Moisture Fluxes*

The surface Bowen ratio is dramatically different for August 20 (0.1 to 0.3) than for the October flights (~4), and the flux profiles are correspondingly different. The sensible heat fluxes are small (Figures 13, 15, and 16) and show reasonable profiles with height. The aircraft moisture fluxes (Figures 14 and 17) are large, and widely scattered. The dashed lines are drawn between the averages of the lowest and highest level runs, but with only three levels and such large scatter, the profiles of moisture flux with height cannot be considered accurate. Once

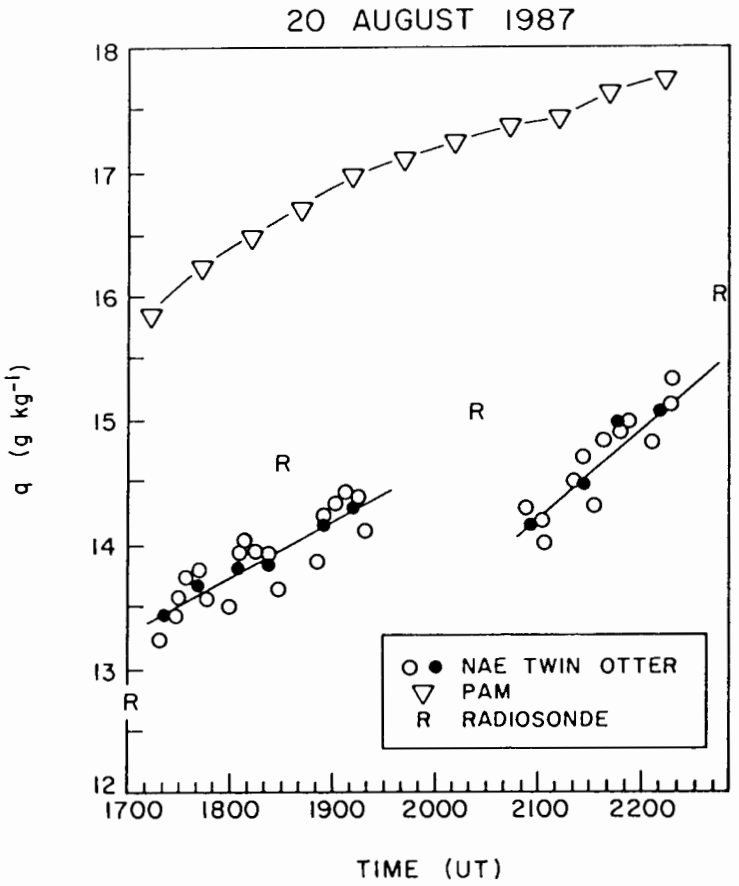

Fig. 12. Changes in mixing ratio with time for measurements on August 20, 1987. See Figure 3 for interpretation of symbols.

again however, the surface mean measurement and budget estimates (S and B) are all above the dashed linear extrapolation of the aircraft to the surface (A).

(iii) *Inversion Level Fluxes*

The inversion height is much lower (500–700 m) than in the two October flights. Figures 13 to 17 also show estimates of the inversion level fluxes. The radiosondes give an average $\beta_1 = -0.4$ (range -0.3 to -0.6), for the morning flights, and -0.28 (range: -0.25 to -0.30) for the afternoon flight. Using the measured surface fluxes of (129, 422 W m^{-2}), (A4a), and (A4b) give $(F_{1\theta}, F_{1q}) = (-39, 98\ \text{W m}^{-2})$ for the morning flights. The corresponding values for the afternoon flight are $(F_{1\theta}, F_{1q}) = -18, 64\ \text{W m}^{-2})$. These inversion-level moisture fluxes are roughly consistent with the profile below, but as in Figures 4, 6 and 9, the θ flux estimates lie above the solid trend line (Figures 13, 15, and 16).

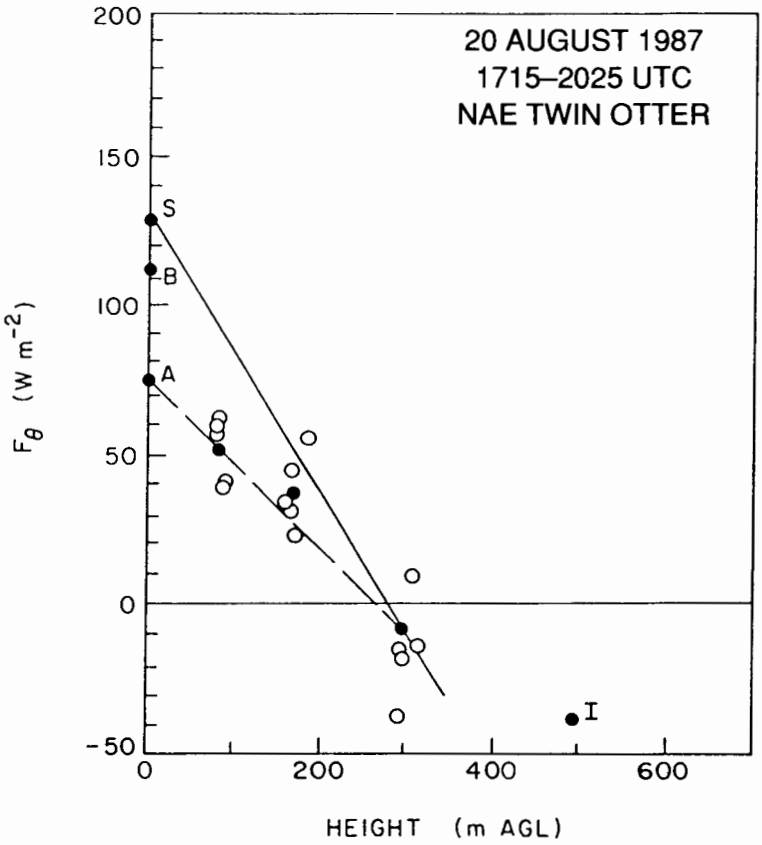

Fig. 13. As in Figure 4, for Twin Otter data from 1715 to 2025 UTC on August 20, 1987.

(iv) *Heat and Moisture Budgets*

Table V shows the heat and moisture budgets for the two morning flights (NAE TW and UW KA) and the afternoon flight (NAE TW). Both the heating of the layer and the vertical flux divergence decrease from the morning to afternoon flights, whereas both components of the θ advection remain almost unchanged during the day, with little net advection. The independent θ budgets from the two aircraft for the two remaining flights agree remarkably well. The budget estimate of the surface θ flux for all three flights (morning and afternoon) lies between the surface measurements and the extrapolated aircraft flux. In the moisture budget from the NAE TW aircraft, there is some dry advection in the morning, so that the moistening of the layer must come from the vertical flux divergence. The scattered aircraft data show little flux divergence with height, so that they do not satisfy the budget. The combination of the higher surface latent heat flux (422 W m^{-2}, Figure 14) and the measured aircraft flux at 300 m satisfies the budget

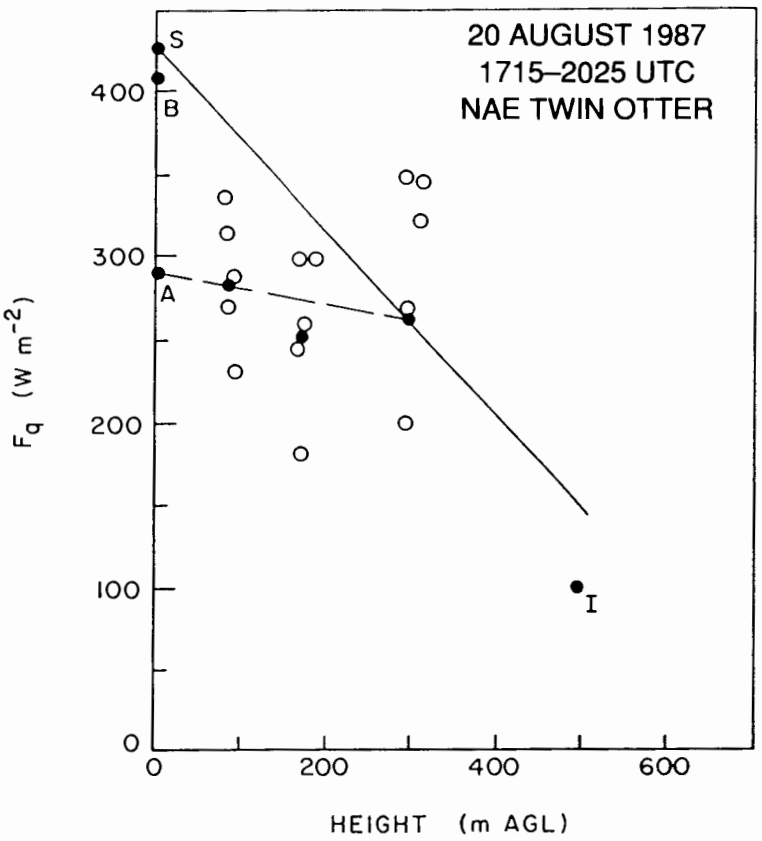

Fig. 14. As in Figure 5, for Twin Otter data from 1715 to 2025 UTC on August 20, 1987.

much better. We conclude that either the aircraft fluxes at low level are too low, or those at the upper level are too high. If we accept the 300 m aircraft fluxes, then the budget gives a surface latent heat flux estimate, $B \approx 405$ W m^{-2}. For the afternoon budget, the fluxes have fallen; but the general pattern with height is unchanged with the gradient with height being a little more clearly defined. There is now net moist advection. The budget gives an estimated surface flux which is much closer to the surface measurements than to the extrapolated aircraft data. The five August budgets consistently show that the aircraft surface flux estimate (A) is the lowest, and the mean surface measurements (S) highest, with the budget estimates (B) in between, usually closer to the surface values. The inversion flux estimates (I) generally support the budget analysis.

5. Summary of Results

Table VI summarizes the surface and inversion level fluxes from the budget analyses presented above.

TABLE V

Heat and moisture budgets for August 20, 1987

(θ Budget ($\bar{\rho}C_p x$)	$\partial\theta/\partial t$	$\bar{u}\,\partial\theta/\partial x$	$\bar{v}\,\partial\theta/\partial y$	Aircraft/surface $\partial(\overline{w'\theta'})/\partial z$	Aircraft/surface Residual	Units
NAE TW (MORNING)	0.393	−0.077	0.086	−0.274/−0.460	0.128/−0.058	W m^{-3}
				Residual as layer flux difference	38/−17	W m^{-2}
				Surface flux (budget/aircraft/surface)	112/74/129	W m^{-2}
UW KA (MORNING)	0.373	−0.074	0.103	−0.332/−0.411	0.070/−0.009	W m^{-3}
				Residual as layer flux difference	24/−3	W m^{-2}
				Surface flux (budget/aircraft/surface)	126/102/129	W m^{-2}
NAE (AFTERNOON)	0.065	−0.055	0.080	−0.080/−0.131	0.009/−0.041	W m^{-3}
				Residual as layer flux difference	3/−13	W m^{-2}
				Surface flux (budget/aircraft/surface)	28/25/41	W m^{-2}
q Budget ($\bar{\rho}L\,x$)	$\partial\bar{q}/\partial t$	$\bar{u}\,\partial\bar{q}/\partial x$	$\bar{v}\,\partial\bar{q}/\partial y$	$\partial(\overline{w'q'})/\partial z$	Residual	
NAE (MORNING)	0.327	0.109	0.051	−0.098/−0.543	0.389/−0.056	W m^{-3}
				Residual as layer flux difference	117/−17	W m^{-2}
				Surface flux (budget/aircraft/surface)	405/288/422	W m^{-2}
NAE (AFTERNOON)	0.583	0.051	−0.152	−0.200/−0.570	0.282/−0.088	W m^{-3}
				Residual as layer flux difference	89/−28	W m^{-2}
				Surface flux (budget/aircraft/surface)	323/234/350	W m^{-2}

Extrapolating the aircraft sensible heat flux at the lowest level (~70 m) to the surface gives average surface sensible heat flux estimates only $61 \pm 6\%$ of the surface flux measurements, which generally agree with the budget estimate of the surface fluxes. For the four NAE Twin Otter flights, this ratio is slightly smaller and very consistent at $58 \pm 3\%$; whereas the UW King Air has 2 higher values with an average of 72%. The cause of this discrepancy between aircraft and surface flux measurements is still not understood, although we discuss some possibilities below. However, these six budget studies suggest that this flux underestimate is a systematic problem for both aircraft, and that the surface tower measurements are more representative of the areal average given by the budget. The difference between surface measurements and the budget estimates is probably not significant: the agreement in means becomes very close if we exclude the October 8 UW KA flight, for which the budget flux estimate is questionable (see 4(a)(iv)).

The latent heat budgets indicate that the extrapolated aircraft surface values

TABLE VI

Summary of surface and inversion fluxes

Date		Surface (Measured, S)	Surface (Extrapolated, A)	Surface (Budget, B)	Inversion (Model, I)
		Sensible heat fluxes ($W m^{-2}$)			
20 Aug.	#29 NAE TW	129	74	112	−39
20 Aug.	#30 NAE TW	41	25	28	−18
20 Aug.	UW KA	129	102	126	−39
8 Oct.	NAE TW	273	161	286	−55
8 Oct.	UW KA	298	194	389	−60
13 Oct.	NAE TW	307	167	320	−81
Mean	196	121	210		
		100%	61% (±6%)	107%	
	NAE TW		58% (±3%)		
	UW KA		72%		
		Latent heat fluxes ($W m^{-2}$)			
20 Aug.	#29	422	288	405	98
20 Aug.	#30	350	234	323	64
8 Oct.		72	61	50	−14
13 Oct.		78	77	79	253
Mean		231	165	212	
		100%	71%	93%	

are also low, about 70% of the surface flux measurements. The difference between the budget estimates and the surface measurements is again probably not significant: for the two cases in October, the surface latent heat flux is small ($<100\ W m^{-2}$) and for both aircraft, surface and budget estimates are within the errors. For the morning August case, the aircraft fluxes do not show a reliable gradient with height, so that this budget is questionable.

The magnitude of the flux underestimation by the aircraft was unexpected. Filtering and inadequate sampling of low frequency contributions to the flux must be responsible for part of the underestimate. The underestimate of the latent heat flux is smaller than for the sensible heat flux, suggesting that part of the sensible heat flux underestimate may be due to flow distortion effects on the temperature fluctuation measurements, as discused by Wyngaard (1988). However, we are still searching for additional causes. FIFE may be one of the first experiments where such an exacting comparison between direct surface flux measurements, aircraft flux measurements and budget estimates could be made.

Considering the problems of measurement on this scale, the six heat and four moisture budgets are very informative. There are clearly problems with the low-level aircraft flux measurements, which are being studied. However, we were encouraged to find that the aircraft data can be used to give such good budget

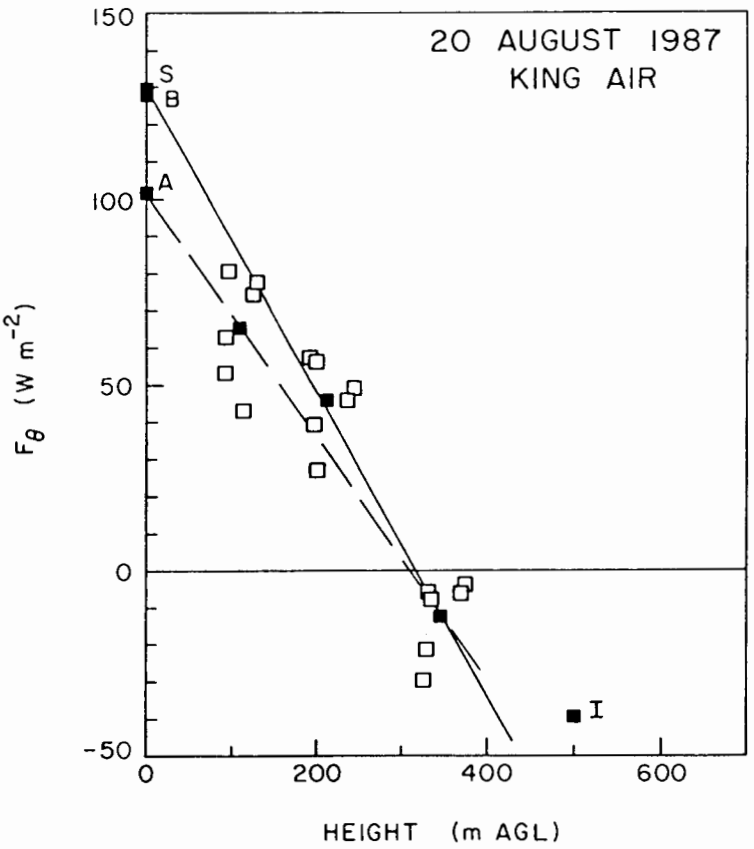

Fig. 15. As in Figure 6, for King Air data 1720 to 1920 UTC on August 20, 1987.

estimates of the areal average surface fluxes, and that these agreed with a simple average of the surface flux measurements. The aircraft can measure the time rate of change in the ABL with high accuracy: they show trends which are close to those of the surface PAM stations up to the times of the surface temperature maxima, but not while the surface subsequently cools. The measurement of the horizontal advection on this scale is not possible from surface stations with different sensors, located over different soil and vegetation types. The measurement of advection by a single aircraft is near the limits of system accuracy, and needs both careful averaging and correction for time changes. However. these budgets suggest that it is possible. One useful improvement would be to double the along-wind separation of the stacks from ~11 to ~22 km. This would double the advection time across the pattern from 15 to 30 min, without increasing significantly the time taken to fly the pattern. The choice of flying the pattern in the sequence shown in Figure 1 to give equal average times at each end was valuable, and minimizes

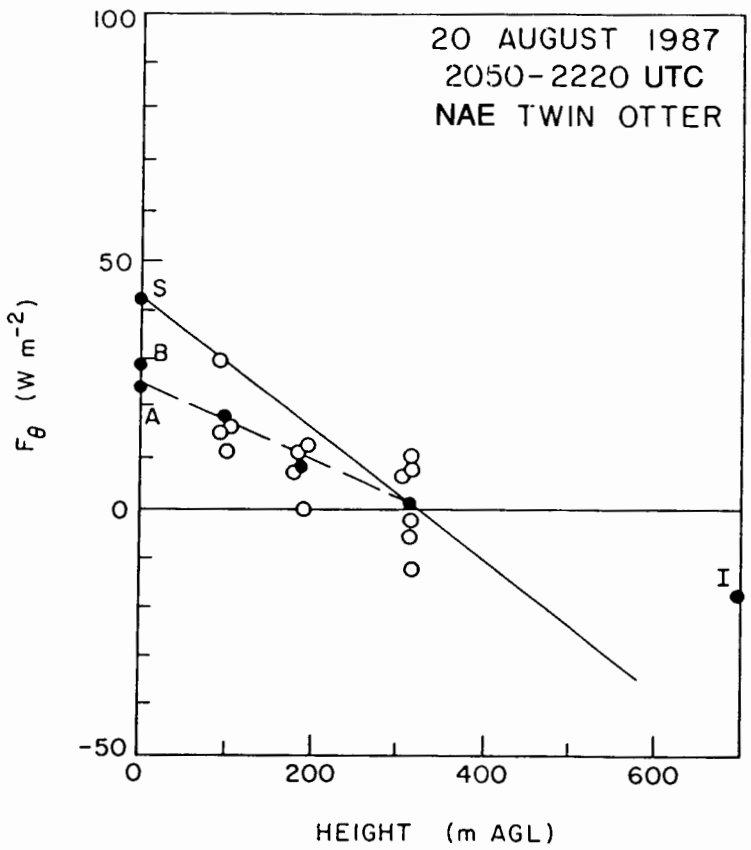

Fig. 16. As in Figure 4, for Twin Otter data from 2050 to 2220 UTC on August 20, 1987.

ferry times between stacks. However, even small differences between mean stack times must be corrected for. Four flight levels are desirable and the presence of clouds should be avoided.

The budgets are generally consistent with mixed boundary-layer theory. The experimental data show nearly well mixed layers with little vertical variation in the time rates of change or horizontal gradients, in agreement with the mixed-layer model approximation. However, they do suggest that the closure parameter k (see Appendix) may be considerably higher than 0.2. Typical entrainment rates at ABL top are $\sim 2\,\mathrm{cm\,s^{-1}}$, but they cannot be estimated accurately from these data.

If advection is ignored (or perhaps reduced by averaging larger data sets with similar diurnal behavior), the model analysis in the Appendix suggests that, in addition to surface measurements, the key upper level parameters are the closure parameter k, and the Bowen ratio at the inversion. The latter can be estimated

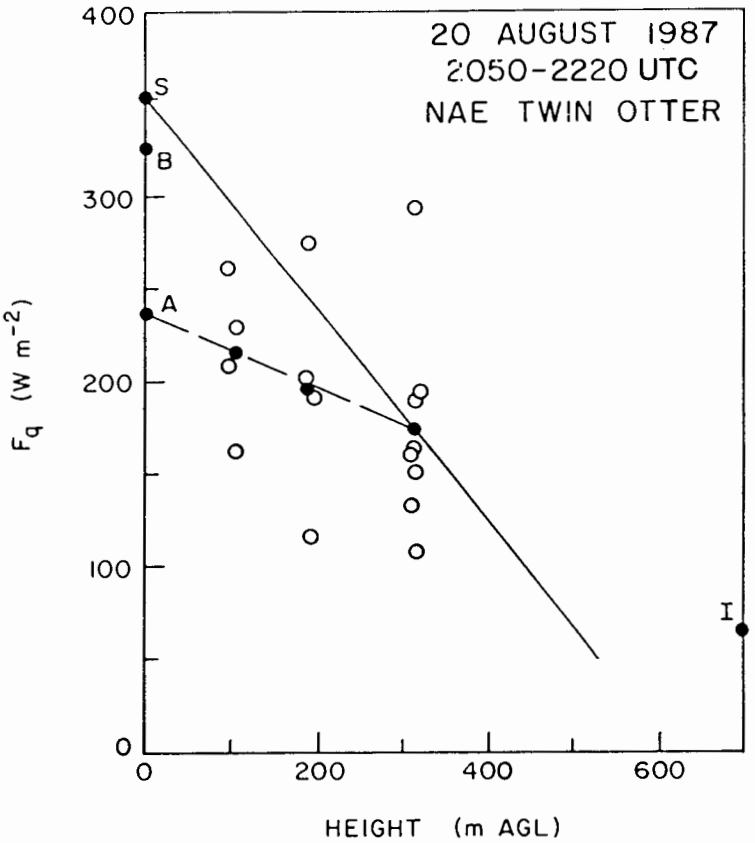

Fig. 17. As in Figure 5, for Twin Otter data from 2050 to 2220 UTC on August 20, 1987.

from aircraft or balloon soundings, but a more careful analysis of ABL growth using sodar or lidar data is needed to estimate k more accurately.

Appendix: Mixed-Layer Model and Inversion-Level Fluxes

Dry mixed-layer models (Betts, 1973; Carson, 1973, Tennekes, 1973), relate the inversion-base virtual heat flux to the surface virtual heat flux,

$$F_{1\theta_v} = -kF_{0\theta_v}, \tag{A1}$$

where $k \approx 0.2$, and F denotes a heat flux in W m^{-2}. The virtual heat fluxes are given by

$$F_{0\theta_v} = F_{0\theta} + \delta\epsilon F_{0q}, \tag{A2a}$$

$$F_{1\theta_v} = F_{1\theta} + \delta\epsilon F_{1q}, \tag{A2b}$$

where $\delta\epsilon = 0.608 C_p T/L = 0.073$. Substituting Bowen ratios at the surface and the inversion

$$\beta_0 = F_{0\theta}/F_{0q}, \tag{A3a}$$

$$\beta_1 = F_{1\theta}/F_{1q}, \tag{A3b}$$

gives, on rearrangement, the inversion-level fluxes

$$F_{1\theta} = -kF_{0\theta}(1 + \delta\epsilon/\beta_0)/(1 + \delta\epsilon/\beta_1), \tag{A3a}$$

$$F_{1q} = F_{1\theta}/\beta_1. \tag{A4b}$$

Given the surface fluxes, the closure parameter k, and the Bowen ratio at the inversion, we can estimate the inversion-level fluxes. The Bowen ratio at the inversion was determined from both aircraft and radiosonde soundings by looking at the slope of $\partial\bar{\theta}/\partial\bar{q}$ across the capping inversion. For dry mixed layers, previous authors have suggested the closure parameter $k \approx 0.2$(Tennekes, 1973; Betts, 1973; Stull, 1976). However, the inversion level heat flux estimates (marked I on the flux figures) all lie above the linear fits (solid lines) between the surface fluxes and the highest level aircraft fluxes, suggesting that $k = 0.2$ may be too small. If we extrapolate the flux gradients $\partial(\overline{w'\theta'})/\partial z$ to the inversion, clearly we can estimate k. Table VII shows these values of k derived from the measured surface fluxes, surface and inversion level Bowen ratios, the flux gradients, $\partial(\overline{w'\theta'})/\partial z$, and the inversion height h. α is the coefficient $(1 + \delta\epsilon/\beta_0)/(1 + \delta\epsilon/\beta_1)$ in (A4a). The mean value is 0.43 ± 0.12. The scatter is probably an underestimate of the uncertainty in k. This is a sensitive calculation since it involves extrapolating the heat flux gradient to a poorly known inversion height. Given errors in the flux gradient of ± 0.03 W m^{-3} (Table II), and h of ± 100 m for the deep ABL's, the error in $F_{1\theta}$ may be as large as ± 50 W m^{-2}. Improvements in the analysis require measurements of mean inversion height and boundary-layer growth rate (such as by lidar or sodar) to constrain the entrainment fluxes better at the inversion. The budget analysis

TABLE VII

Estimates of k from flux divergence

Flight		$F_{0\theta}$ W m^{-2}	$\bar{\rho}C_p\partial(\overline{w'\theta'})$ W m^{-3}	$h/\partial z$ m	$F_{1\theta}$ W m^{-2}	α	k
Aug. 20	#29 NAE TW	129	−0.461	500	−101	1.51	−0.52
	#30 NAE TW	41	−0.131	700	−51	2.12	−0.57
Aug. 20	UW KA	130	−0.411	500	−76	1.51	−0.39
Oct. 8	#36 NAE TW	273	−0.392	1050	−139	1	−0.51
Oct. 8	UW KA	298	−0.406	1000	−108	1	−0.36
Oct. 13	#41 NAE TW	307	−0.478	850	−99	1.32	−0.25
						Mean	−0.43 (±0.12)

does, however, suggest that the closure parameter k may be larger than 0.2 for these high wind regimes.

Acknowledgements

A. K. Betts was supported by NASA-GSFC under Contract NAS5-30524, and NSF under Grant ATM87-05403. R. L. Desjardins and J. I. MacPherson gratefully acknowledge funding from NASA, the National Research Council and Agriculture Canada for their participation in FIFE 87. The assistance of the staff of NAE of NRC for collecting the data is also acknowledged. R. D. Kelly was supported by NASA-GSFC under Contract NAG-5-913. He wishes to thank E. Gasaway, G. Gordon, and K. Chartier for their efforts in the field, and S. Allen for drafting the figures. The enthusiastic cooperation of *all* FIFE participants is gratefully acknowledged.

References

Benech, B., Durand, P., and Druilhet, A.: 1987, 'A Case Study of a Non-homogeneous Boundary Layer (AUTAN 84 Experiment)', *Ann. Geophys.* **5B**, 451–460.

Betts, A. K.: 1973, 'Non-precipitating Cumulus Convection and its Parameterization', *Quart. J. Roy. Meteorol. Soc.* **99**, 178–196.

Budak, A.: 1974, *Passive and Active Network Analysis and Synthesis*, Houghton Mifflin Co., Boston, 733 pp.

Carson, D. J.: 1973, 'The Development of a Dry Inversion-Capped Convectively Unstable Boundary Layer', *Quart. J. Roy. Meteorol. Soc.* **99**, 450–467.

Desjardins, R. L., Brach, E. J., Alvo, P., and Schuepp, P. H.: 1982, 'Aircraft Monitoring of Surface Carbon Dioxide Exchange', *Science* **216**, 733–735.

Desjardins, R. L., MacPherson, J. I., Alvo, P., and Schuepp, P. H.: 1986, 'Measurements of Turbulent Heat and CO_2 Exchange over Forests from Aircraft', in B. A. Hutchison and B. B. Hicks (eds.), *The Forest-Atmosphere Interaction*. Reidel Publ., Dordrecht, pp. 645–658.

Desjardins, R. L., MacPherson, J. I., Betts, A. K., Schuepp, P. H., and Grossman, R.: 1988, 'Diverence of CO_2, Latent and Sensible Heat Fluxes: A Case Study', *Proceedings on Lower Tropospheric Profiling: Needs and Technologies*, Boulder, CO, pp. 71–72.

Desjardins, R. L., MacPherson, J. I., and Schuepp, P. H.: 1989a, 'Long Wavelength Contribution to Aircraft-Based Flux Estimates of CO_2, H_2O and Sensible Heat', *19th Conf. on Agriculture and Forest Meteorology, Charleston, NC. AMS*, March 7–10, pp. 125–128.

Desjardins, R. L., MacPherson, J. I., Schuepp, P. H., and Karanja, F.: 1989b, 'An Evaluation of Airborne Eddy Flux Measurements of CO_2, Water Vapor and Sensible Heat', *Boundary-Layer Meteorol.* **47**, 55–69.

Jacquot, R. G.: 1981, *Modern Digital Control Systems*, Marcel Dekker, Inc., New York, 355 pp.

Lenschow, D. H.: 1970, 'Airplane Measurements of Planetary Boundary Layer Structure', *J. Appl. Meteorol.* **9**, 874–884.

Lenschow, D. H.: 1986, 'Aircraft Measurements in the Boundary Layer', in D. H. Lenschow (ed.), *Probing the Atmospheric Boundary Layer. Amer. Meteorol. Soc.*, pp. 39–55.

Lenschow, D. H., Pearson, R., and Stankov, B. B.: 1981, 'Estimating the Ozone Budget in the Boundary Layer by Use of Aircraft Measurements of Ozone Eddy Flux and Mean Concentration', *J. Geophys. Res.* **86**, 7291–7297.

MacPherson, J. I., Desjardins, R. L., Brach, E., Alvo, P., and Schuepp, P. H.: 1985, 'Preliminary Evaluation of Aircraft Mounted Sensors for Gaseous Exchange Measurements', *17th Conf. on Agric. and Forest Meteorol.*, Phoenix, AZ., pp. 13–17.

Sellers, P. J., Hall, F. G., Asrar, G., Strebel, D. E., and Murphy, R. E.: 1988, 'The First ISLSCP Field Experiment (FIFE)', *Bull Amer. Meteorol. Soc.* **69**, 22–27.

Stull, R. B.: 1976, 'The Energetics of Entrainment Across a Density Interface', *J. Atmos. Sci.* **33**, 1260–1267.

Tennekes, H.: 1973, 'A Model for the Dynamics of the Inversion above a Convectlve Boundary Layer', *J. Atmos. Sci.* **30**, 558–567.

Webb, E. K., Pearman, G. I., and Leuning, R.: 1980, 'Correction of Flux Measurements for Density Effects due to Heat and Water Vapour Transfer', *Quart. J. Roy. Meteorol. Soc.* **106**, 85–100.

Wyngaard, J. C.: 1988, 'The Effects of Probe-induced Flow Distortion on Atmospheric Turbulence Measurements: Extension to Scalars', *Boundary-Layer Meteorol.* (in press).